

# Charge carrier interaction with a purely electronic collective mode: Plasmarons and the infrared response of elemental bismuth

Riccardo Tediosi,<sup>1</sup> N. P. Armitage,<sup>1,2</sup> E. Giannini,<sup>1</sup> and D. van der Marel<sup>1</sup>

<sup>1</sup>*Département de Physique de la Matière Condensée, Université de Genève,  
quai Ernest-Ansermet 24, CH1211 Genève 4, Switzerland.*

<sup>2</sup>*Department of Physics and Astronomy, The Johns Hopkins University, Baltimore, MD 21218, USA.*

(Dated: October 29, 2018)

We present a detailed optical study of single crystal bismuth using infrared reflectivity and ellipsometry. Colossal changes in the plasmon frequency are observed as a function of temperature due to charge transfer between hole and electron Fermi pockets. In the optical conductivity, an anomalous temperature dependent mid-infrared absorption feature is observed. An extended Drude model analysis reveals that it can be connected to a sharp upturn in the scattering rate, the frequency of which exactly tracks the temperature dependent plasmon frequency. We interpret this absorption and increased scattering as the first direct optical evidence for a charge carrier interaction with a collective mode of purely electronic origin; here electron-plasmon scattering. The observation of a *plasmaron* as such is made possible only by the unique coincidence of various energy scales and exceptional properties of semi-metal bismuth.

PACS numbers: 71.45.-d, 78.40.Kc, 78.20.-e, 78.30.-j

Elemental semi-metals, such as graphite and bismuth, are materials of much long term interest due to their exceptional properties, including large magnetoresistive and pressure dependent effects [1, 2, 3]. In the case of bismuth these properties derive from its low carrier number, ( $\approx 10^{-5}$  electrons per atom), reduced effective masses ( $\approx 10^{-2}$  electron masses), small Fermi wavevector ( $\approx 40$  nm), long mean free path ( $\approx 1$  mm), and large high frequency dielectric constant ( $\epsilon_{\infty} \approx 100$ ).

A number of recent results are causing an increased interest in these materials, both from the side of fundamental solid-state physics as well as applications potential. For instance a field dependent crossover reminiscent of the 2D metal/insulator transition in MOSFETs [4] has been observed in both graphite and bismuth [5]. Isolated single layers of graphene have been shown to have novel transport properties and an anomalous quantization of the Quantum Hall effect resulting from their low carrier number and exceptional zero mass Dirac cone dispersion relation [6, 7]. Moreover there continues to be interest in bismuth for studies of quantum confinement [8]. On the technical side, advances in film growth [9], anomalously long spin diffusion lengths and very large magnetoresistive response makes bismuth useful for possible incorporation in nanomagnetometers, magneto-optical devices and spintronics applications [10, 11, 12, 13].

In principle transport phenomena in bismuth should be well described by the conventional theory of metals, but due to its exceptional parameters, there are substantial departures from standard metallic behavior. For instance, electronic energy scales, like the Fermi energy, are very low giving strongly temperature dependent effective masses and charge densities. Moreover, the material's very low carrier density opens up the possibility - at least in principle - for novel plasmonic effects and

strong electron-electron interactions due to the relative scales between potential and kinetic energy at low charge densities [14].

Despite the scientific and technological interest in bismuth, its optical and infrared properties have been under-investigated. In this letter we present detailed temperature dependent optical measurements over the full optical range from FIR to UV of single crystal bismuth. We observe a narrow Drude peak which has a plasma frequency value consistent with the low carrier number. Colossal changes in the plasma frequency are observed as a function of temperature, due to charge transfer between electron and hole pockets. We find an anomalous mid-infrared absorption in the real part of the conductivity. An extended Drude model analysis reveals that the scattering rate has an abrupt onset at a temperature dependent energy scale which is found to be almost exactly coincident with the independently measured plasmon energy. This is the first direct optical observation of a strongly coupled electron-plasmon elementary excitation - a *plasmaron*.

Single crystal bismuth was grown by a modified Bridgman-Stockbarger technique in a vertical three-zone furnace. A silica tube was filled with  $\sim 5$  grams of 99.999% pure Bi powder (Cerac) and sealed under vacuum. The ampoule was held vertically in a three-zone furnace and annealed above the melting point of Bi ( $T_m = 271.4$  °C) for 10 hours before decreasing the temperature at a rate of 30 °C/h, while keeping a temperature gradient of 10-15 °C/cm. The crystals were cleaved from the as-grown boule along a plane perpendicular to the trigonal direction [001] at LN<sub>2</sub> temperatures. X-ray powder diffraction revealed that the mirror-like cleavage surfaces were [110] planes perpendicular to the trigonal axis which were subsequently used as reflecting surfaces

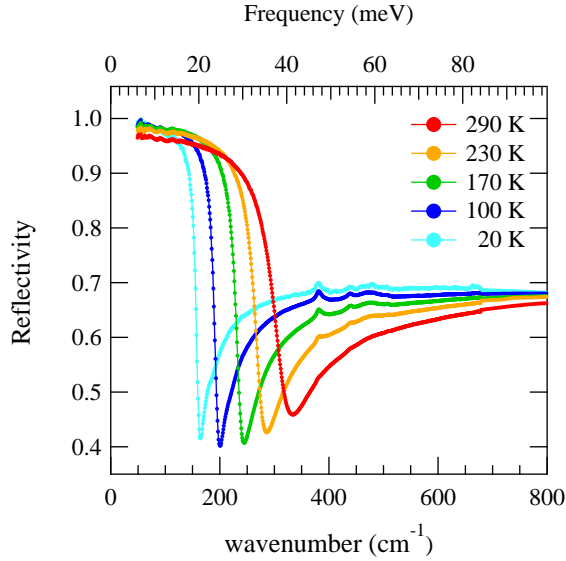


FIG. 1: (color online) Single-crystal bismuth reflectivity vs wavenumber ( $\omega/2\pi c$ ) for temperature  $T = 290$  (red), 230 (orange), 170 (green), 100 (blue) and 20 K (cyan). The pronounced shifting of the minimum in the range  $180 - 350 \text{ cm}^{-1}$  represents the position of the screened plasma frequency  $\omega_p^*$ . The small peak around  $380 \text{ cm}^{-1}$  is an experimental artifact due to a small nonlinearity in a strong absorption of the interferometer's beam splitter.

for optical experiments.

We measured the DC resistivity and optical spectra in the frequency range from  $50 \text{ cm}^{-1}$  ( $6.2 \text{ meV}$ ) to  $30000 \text{ cm}^{-1}$  ( $3.8 \text{ eV}$ ) combining infrared (IR) reflectivity via FT spectroscopy and ellipsometry in the VIS-UV energy range. In the IR experiment the sample was mounted in a quasi-normal incidence configuration ( $\theta_{\text{inc}} = 11^\circ$ ) and reflected signal intensity was recorded during slow temperature scans in the temperature range from 290 K down to 20 K with a resolution of approximately 1 K. The absolute value of the reflectivity  $R(\omega, T)$  was calculated using a reference gold layer evaporated *in situ* on the sample surface.

In Fig. 1 the reflectivity is presented for five selected temperatures in the far-infrared spectral range. A spectacular shift of the reflectivity edge from around  $333 \text{ cm}^{-1}$  at room temperature to a value of  $164 \text{ cm}^{-1}$  at 20 K indicates a strong reduction of the plasmon frequency with cooling. This derives from a change in density due to thermal charge transfer from electron to hole pockets. The small feature present at  $380 \text{ cm}^{-1}$  at all temperatures is a non-linear effect of the detector as a result of absorption in the beamsplitter and is not an intrinsic feature of bismuth. The ellipsometry and IR data were combined using a Kramers-Kronig consistent variational fitting procedure [15]. This allows the extraction of all the significant frequency and temperature dependent optical properties like for instance, the complex conduc-

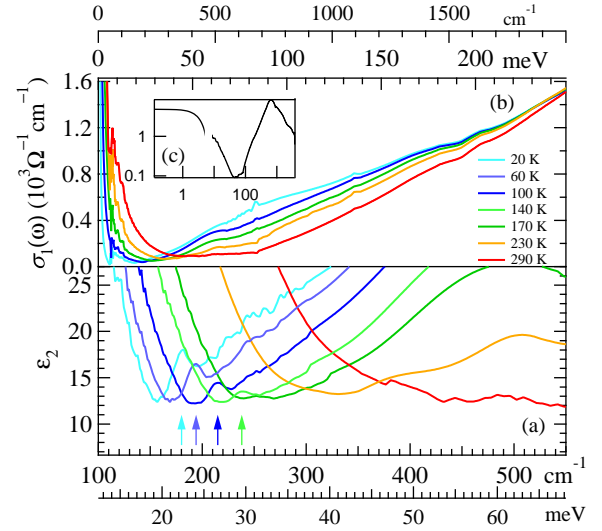


FIG. 2: (color online) (a) Optical conductivity derived from Kramer-Kronig analysis for selected temperatures. (b) The imaginary dielectric constant  $\epsilon_2$  over a much smaller energy range that emphasizes the remarkable prepeak structure. (c) Log-Log scale plot of  $\sigma_1(\omega)$  for  $T = 290 \text{ K}$ , units are meV.

tivity  $\hat{\sigma}(\omega, T) = \sigma_1 + i\sigma_2$ . Note that although it does not affect our conclusions either way, the  $380 \text{ cm}^{-1}$  artifact has been removed from the data used to generate the plots in subsequent figures. The extended frequency range and ellipsometry used in our experiment allows us to extract more accurate parameter values from the subsequent analysis than what has been reported in previous work [16] where just the FIR spectral range was analyzed.

In Fig. 2(a) the optical conductivity  $\sigma_1(\omega)$  is presented for corresponding data of Fig. 1 in the FIR-MIR range. The plot reveals two main features developing with decreasing temperature; the first is a progressive narrowing of the Drude peak from an half-width-half-maximum value of  $42.3 \text{ cm}^{-1}$  at room temperature down to a value of  $3.3 \text{ cm}^{-1}$  at 20 K. Additionally, we observe a dramatic appearance and strengthening of an absorption centered around  $700 \text{ cm}^{-1}$  and characterized by an onset approximately around  $350 \text{ cm}^{-1}$  at room temperature which appears to shift downward as the temperature is lowered. In the inset to Fig 2 the conductivity is presented over the full measurement range at room temperature; a prominent peak is evident in the figure centered around  $5500 \text{ cm}^{-1}$  whose energy and temperature dependence are compatible with the direct interband transition at the  $L$ -symmetry point.

While the narrowing of the Drude peak is typical behavior for a metal whose DC conductivity increases at lower temperatures as a consequence of the reduction of the scattering processes, the appearance of an MIR absorption is unusual. In fact, a closer look shows an even more interesting aspect, as shown in Fig. 2b where we plot a greatly expanded view of the related quantity, the

imaginary dielectric constant  $\epsilon_2 = 4\pi\sigma_1/\omega$ ; the low energy onset of this MIR absorption feature is preceded by a small, but distinct and temperature dependent *prepeak* absorption structure.

In a previous study, the MIR absorption has been assigned to the threshold for direct interband transitions at the  $L$  point [16]. Certainly interband transitions play a role in part of this energy range, but the energy scale of the onset and prepeak are not quite right for them to be the entire contribution. The interband gap reported at low temperature is 13.7 meV [3] and combined with an  $L$  point Fermi energy  $E_F$ , gives a minimum threshold for direct absorption of  $E_c + 2E_F$  of 67.1 meV ( $540 \text{ cm}^{-1}$ ), which is much bigger than the onset. The discrepancy even increases at low temperature where the onset falls to  $125 \text{ cm}^{-1}$ . It is possible that the region of the absorption onset is partially affected by an indirect interband phonon coupled process, as recently proposed for a similar absorption in bismuth nanowires [17]. Although this process has been investigated theoretically [18, 19] we observe that our experimental data deviate considerably from the expectations, in particular in the region where the prepeak appears. In the rest of this work we will thus concentrate on the explanation that such anomaly derives from an electron-plasmon interaction.

In Fig 3, we analyze the complex conductivity data in terms of an extended Drude model. We extract the frequency dependent scattering rates  $\tau^{-1}(\omega)$  and effective masses  $m^*(\omega)$  via the relations

$$\begin{aligned} \tau^{-1}(\omega) &= -(\omega_p^2/\omega) \text{Im}(\epsilon(\omega) - \tilde{\epsilon}_\infty)^{-1} \\ m^*(\omega)/m_e &= -(\omega_p^2/\omega^2) \text{Re}(\epsilon(\omega) - \tilde{\epsilon}_\infty)^{-1} \end{aligned} \quad (1)$$

where  $\omega_p$  is the plasma frequency and  $\tilde{\epsilon}_\infty$  represents the temperature dependent interband contribution to the dielectric constant. We should stress here the fact that the extended Drude model is strictly valid only in the region where interband transitions do not play a major role. We see in Fig. 3 that the data is relatively well described at the lowest frequencies within the usual Drude framework where the scattering rates and masses are frequency independent over roughly the same frequency interval. However we observe a sharp onset in the scattering rate at a well-defined temperature dependent energy scale. This reflects the MIR absorption pointed out previously and makes  $\tau^{-1}(\omega)$  deviate from the constant value expected from a simple Drude model.

As noted earlier, according to band structure parameters [20] the position of the scattering onset  $\omega_\tau$  is too high to derive from a direct interband process. In fact, the temperature dependence of this absorption's onset and prepeak is reminiscent of the large temperature dependence of the plasma frequency itself. We observe that the onset almost exactly tracks the independently measured plasma frequency as a function of temperature, as shown in the parametric plot Fig. 4(a) where we plot the

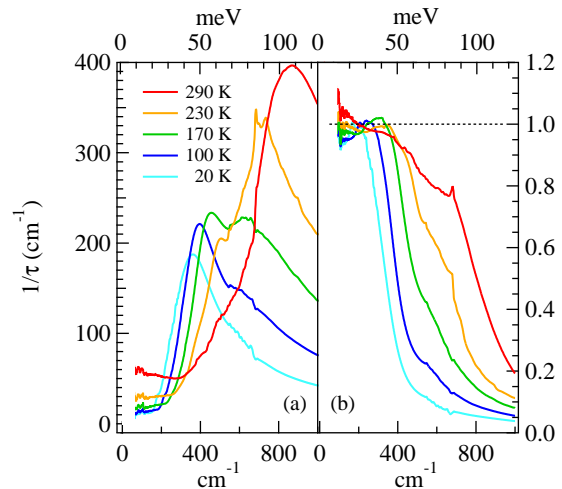


FIG. 3: (color online) Extended-Drude analysis results: (a) the low frequency scattering rate  $\tau^{-1}(\omega)$  progressively falls as the temperature is lowered. An approximately frequency independent region is interrupted by a sharp onset in scattering. (b) The effective mass  $m^*(\omega)/m$  is flat as over a similar range.  $m$  is defined as the band-mass of the carrier for the specific crystal orientation used.

frequency of this onset or “kink” in the  $\epsilon_2(\omega)$  function  $\omega_\tau$  vs.  $\omega_p^*$  as defined by the zero crossing of the experimental  $\epsilon_1(\omega)$  and the onset is defined by the energy position of the prepeak’s half maximum on its low frequency side. Based on this parametric plot in Fig. 4 we can conclusively identify the plasma frequency as setting the energy scale for the observed absorption process. The plasmon energy changes by almost a factor of two over almost the entire frequency range, but continues to set the scale for the increased scattering throughout.

Due to its longitudinal character, direct excitation of a plasmon by an incident electromagnetic wave is generally not possible. However, a number of scenarios may exist to induce an electron-plasmon coupling effect. Previously, an explanation for the appearance of the MIR peak has been given in terms of an impurity-mediated electron-plasmon coupling [21, 22, 23, 24]. It was proposed that enhanced electron-charged impurity scattering is found near  $\omega_p$  due to the divergence of  $1/\epsilon$ . Although our data are in qualitative agreement with such a scenario, the model used by Gerlach *et al.* [22] has a quantitative agreement only by considering an exceptionally large charged impurity concentration ( $N = 1.5 \times 10^{19} \text{ cm}^{-3}$ ). This is approximately two orders of magnitude greater than the carrier concentration itself and implies a *charged* impurity concentration of 1 part in  $10^4$ , which we consider to be unrealistic considering the high purity of our samples.

In contrast, we propose that we are observing the excitation of plasmons via a decay channel of the excited

electron-hole pairs. This interaction is essentially identical to that considered in the context of electron - phonon [25] or electron - magnon interactions [26]. Such an interaction may in fact be captured within the same Holstein Hamiltonian that is used to describe the electron - longitudinal phonon coupling to treat polarons and so this collective excitation has been called a *plasmaron* [27, 28] in theoretical treatments. Such an excitation is only possible optically in a system where translational symmetry has been broken first by, for instance, Umklapp scattering or disorder that moves oscillator strength to a frequency region near the plasmon energy. In normal metals such an interaction is completely unobservable as the plasmon energy scales are many orders of magnitude higher than transport ones. This is, to the best of our knowledge, the first unambiguous observation of charge carrier scattering with a collective bosonic mode of purely electronic origin.

The possibility also exists that we are observing not an electron-hole decay channel, but instead a direct 3 body excitation of an electron-hole pair and a plasmon with a net momentum  $q \sim 0$ . Such processes are possible by going beyond the usual RPA and considering electron-electron interactions (electron-plasmon in the present case) mediated by the crystal potential [14]. In the case of a translational invariant system, the standard Landau-Fermi liquid treatment holds since the photon-induced electron-hole pair are momentum conserving processes. Introducing symmetry breaking terms, like strong Umklapp scattering or disorder, makes such 3 body processes possible. Experimentally this effect may be directly observable using optical spectroscopy since the longitudinal collective mode would be partially coupled to a transverse one [29].

Within the electron-hole plasmon decay channel scenario one might try to model the scattering rate using an expression for the plasmon density of states  $D(\omega)$  and a simple scheme for coupling of the spectrum to electronic excitations [25, 26]. Unfortunately, although aspects of our data are qualitatively consistent with such a scenario, such a calculation is hard to compare with the data exactly, due to the onset of the interband contribution. The low energy prepeak structure is interesting and is *not* captured within any simple models. We speculate that it is a resonant effect due to enhanced electronic interaction near  $\omega_p$  deriving from the divergence of  $1/\epsilon$ .

In view of these difficulties, we show in Fig. 4(b) the 20 K electron energy loss function  $EEL(\omega) = \text{Im} \{-\epsilon^{-1}(\omega)\}$  which should be relatively insensitive to the contributions of interband terms. The plot presents a prominent peak centered at  $\omega_p^*$  but also an high frequency shoulder. The total EEL function can be decomposed using two lorentzian oscillators; one centered at the screened plasma frequency  $\omega_p^* = 160.7 \text{ cm}^{-1}$  with a width  $\gamma_1 = 5.74 \text{ cm}^{-1}$  and another one at  $\omega_2 = 176.4 \text{ cm}^{-1}$  with  $\gamma_2 = 15.6 \text{ cm}^{-1}$ . The position of this latter peak corre-

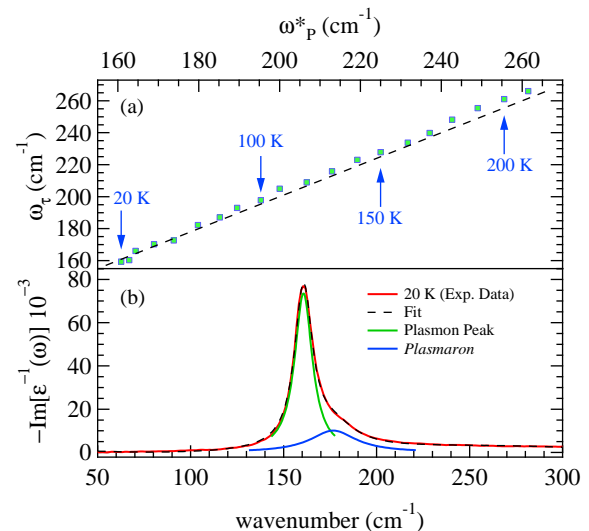


FIG. 4: (color online) (a) A parametric plot  $\omega\tau$  vs.  $\omega_p^*$  shows a slope of 1 supporting the hypothesis of an electron-plasmon interaction. (b) The 20K electron energy loss (EEL) function (red) presents the main plasmon peak and a *plasmaron* peak appearing as a shoulder of the main one.

sponds exactly to the position of the absorption feature seen in  $\epsilon_2(\omega)$  thus demonstrating its admixture of longitudinal plasmonic character.

In conclusion we have made the first optical observation of an electron-plasmon interaction - a *plasmaron*. This observation is made possible only by the low carrier density in Bi, a very large  $\epsilon_\infty$ , and a lack of optically active phonons. This work raises various questions about how these renormalization effects feed back on the low energy properties of this material. It is possible that reducing the charge density further, perhaps through the application of pressure, may enhance such interactions and drive the system into an anomalous metallic state. Pressure dependent optical studies may prove to be a useful probe in this regard. It would also be interesting to search for similar effects in other semi-metals like graphite or single-layer graphene.

The authors would like to thank M. Dressel, H.D. Drew and A.J. Millis for various illuminating conversations. The work at the University of Geneva is supported by the Swiss National Science Foundation through the National Center of Competence in Research “MaNEP”. NPA has been also supported via the NSF’s International Research Fellows program.

- 
- [1] N. B. Brandt *et al.*, Soviet Physics JEPT **20**, 301 (1965).
  - [2] D. Balla and N. B. Brandt, Soviet Physics JEPT **20**, 1111 (1965).
  - [3] V. S. Édel'man, Adv. in Phys. **25**, 555 (1976).
  - [4] S. V. Kravchenko, D. Simonian, M. P. Sarachik, A. D.

- Kent, and V. M. Pudalov, Phys. Rev. B **58**, 3553 (1998).
- [5] X. Du, S. W. Tsai, D. L. Maslov, and A. F. Hebard, Phys. Rev. Lett. **94**, 166601 (2005).
  - [6] K. S. Novoselov *et al.*, Nature **438**, 197 (2005).
  - [7] Y. Zhang *et al.*, Nature **438**, 201 (2005).
  - [8] Y. F. Komnik *et al.*, JETP, Sov. Phys. **33**, 364 (1971).
  - [9] F. Y. Yang *et al.*, Science **284**, 1335 (1999).
  - [10] B. K. Chong *et al.*, J. Vac. Sci. Technol. A **19**, 1769 (2001).
  - [11] G. Boero, M. Demierre, P. A. Besse, and R. S. Popovic, Sensors and Actuators A: Physical **106**, 314 (2003).
  - [12] W. J. Grande, S. Reznik, and J. Ertel, Magnetics IEEE Transactions **33**, 3394 (1997).
  - [13] K. I. Lee *et al.*, Phys. Stat. Sol. B **241**, 1510 (2004).
  - [14] G. Mahan, *Many Particle Physics* (Kluwer Academic, 3rd ed., 2000).
  - [15] A. B. Kuzmenko, Rev. Sci. Instrum. **76**, 083108 (2005).
  - [16] W. S. Boyle and A. D. Brailsford, Phys. Rev. **120**, 1943 (1960).
  - [17] M. R. Black, P. L. Hagelstein, S. B. Cronin, Y. M. Lin, and M. S. Dresselhaus, Phys. Rev. B **68**, 235417 (2003).
  - [18] N. P. Stepanov, Russian Physics Journal **47**, 262 (2004).
  - [19] R. Tediosi, N. P. Armitage, E. Giannini, and D. van der Marel, to be published (2007).
  - [20] M. P. Vecchi and M. S. Dresselhaus, Phys. Rev. B **10**, 771 (1974).
  - [21] E. Gerlach and M. Rautenberg, Phys. Stat. Sol. B **65**, K13 (1974).
  - [22] E. Gerlach *et al.*, Phys. Stat. Sol. B **75**, 553 (1976).
  - [23] L. M. Claessen, A. G. M. Jansen, and P. Wyder, Phys. Rev. B **33**, 7947 (1986).
  - [24] J. Mycielski and A. Mycielski, Phys. Rev. B **18**, 1859 (1978).
  - [25] F. Marsiglio, J. P. Carbotte, and E. Schachinger, Phys. Rev. B **65**, 014515 (2001).
  - [26] J. Carbotte, E. Schachinger, and D. N. Basov, Nature **401**, 354 (1999).
  - [27] B. Lundqvist, Phys. Kondens. Materie **6**, 193 (1967).
  - [28] B. Lundqvist, Phys. Stat. Sol. **32**, 273 (1969).
  - [29] M. Turlakov, J. of Physics A **36**, 9399 (2003).